

Upregulation of CXCL10 in Human Dorsal Root Ganglia during Experimental and Natural Varicella-Zoster Virus Infection[∇]

Megan Steain,^{1,2,†} Kavitha Gowrishankar,^{2,†} Michael Rodriguez,³
Barry Slobedman,^{2,†} and Allison Abendroth^{1,2,†,*}

Department of Infectious Diseases and Immunology, The University of Sydney, Australia¹; The Centre for Virus Research, Westmead Millennium Institute, Sydney, Australia²; and Department of Forensic Medicine, Sydney South West Area Health Service, Sydney Australia³

Received 27 August 2010/Accepted 14 October 2010

Varicella-zoster virus (VZV) reactivation causes herpes zoster, which is accompanied by an influx of lymphocytes into affected ganglia, but the stimulus for this infiltrate is not known. We report that VZV infection of ganglia leads to increased CXCL10 production *in vitro*, in an explant ganglion model and in naturally infected dorsal root ganglia (DRG) during herpes zoster. Lymphocytes expressing the receptor for CXCL10, CXCR3, were also observed throughout naturally infected ganglia during herpes zoster, including immediately adjacent to neurons. This study identifies VZV-induced CXCL10 as a potential driver of T lymphocyte recruitment into DRG during herpes zoster.

Varicella-zoster virus (VZV) establishes latency in sensory ganglia, mainly dorsal root ganglia (DRG) (2, 13, 18), and can reactivate to cause herpes zoster (3). Studies of postmortem ganglia from patients with herpes zoster near the time of death have shown infiltration of these ganglia by immune cells (9), largely T cells (5). However, the cytokines and chemokines which may be responsible for this inflammatory infiltrate are unknown. The chemokine CXCL10 specifically binds to CXCR3 on memory T cells and NK cells to induce migration (11, 21). Neurons and their supporting cells are capable of producing CXCL10 (14), and the expression of CXCL10 during a number of viral infections of the nervous system, including herpes simplex virus encephalitis, rabies, West Nile fever, and dengue, has been reported (7, 8, 15, 17). Therefore, we sought to determine whether VZV replication in human DRG alters the expression of CXCL10 as a potential driver of the immune cell infiltration observed in DRG during herpes zoster.

VZV is highly species specific, and so the whole-explant fetal DRG model which we previously described (4) provides a platform to study the innate immune response to VZV infection within intact human DRG. Furthermore, access to ganglia obtained postmortem from patients suffering from herpes zoster at the time of death allows for comparisons of our *in vitro* model to natural reactivation. In the present study, CXCL10 production was assessed in experimentally infected human explant ganglia as well as in rare naturally infected ganglia removed from a patient with herpes zoster at the time of death.

For experimental VZV infection, human fetal DRG were harvested, explanted, and infected with VZV S as previously described (4). DRG were formalin fixed and paraffin embed-

ded at 24 and 48 h postinfection (p.i.). Productive infection of DRG was confirmed by immunostaining for VZV proteins as described previously (4) (data not shown). Mock- and VZV-infected explant DRG from the same donor were also harvested for RNA extraction, and quantitative reverse transcription-PCR (qRT-PCR) was performed for CXCL10 and normalized to glyceraldehyde-3-phosphate dehydrogenase (GAPDH) as described previously (19). Primer sequences are listed in Fig. 1A. At both 24 and 48 h p.i., CXCL10 mRNA was significantly upregulated ($P < 0.05$) within VZV-infected

A

Primer name		Sequence
CXCL10	Forward	5'-CCAATTTTGTCCACGTGTTG-3'
	Reverse	5'-GCTCCCTCTGGTTCCAAGG-3'
GAPDH	Forward	5'-TCACCAGGGCTGCTTTTAAC-3'
	Reverse	5'-GACAAGCTTCCCGTTCTCAG-3'

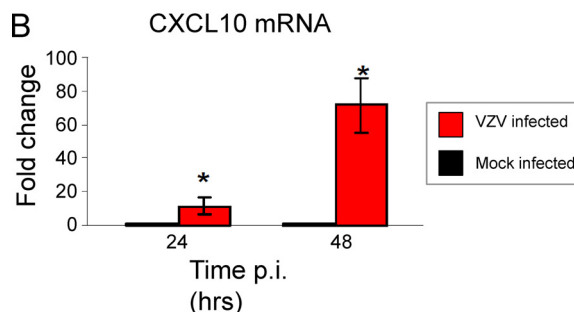


FIG. 1. CXCL10 mRNA levels in human ganglia experimentally infected with VZV. CXCL10 mRNA levels in mock- and VZV-infected ganglia were determined by qRT-PCR and normalized to GAPDH. (A) Forward and reverse primer sequences are shown. (B) The relative quantity of CXCL10 transcripts is represented as a fold change in VZV-infected ganglia in comparison to mock infection. Error bars represent standard error of the mean from three independent experiments using different ganglia samples. Significant difference from the mock-infected control was determined using a one-tailed, paired Student's *t* test (*, $P < 0.05$).

* Corresponding author. Mailing address: Department of Infectious Diseases and Immunology, The University of Sydney, New South Wales, Australia 2006. Phone: 61 2 93516867. Fax: 61 2 93513968. E-mail: allisona@med.usyd.edu.au.

† M.S. and K.G. contributed equally to this work. A.A. and B.S. are co-senior authors who contributed equally.

[∇] Published ahead of print on 27 October 2010.

DRG compared to mock-infected DRG (Fig. 1B). At 24 h p.i., a 15-fold increase in CXCL10 transcript levels over mock DRG was observed, and this increased to 70-fold at 48 h p.i.

We next determined if VZV infection of DRG increased CXCL10 protein secretion. Supernatants from mock- and VZV-infected DRG cultures were harvested at 48 h ($n = 1$), 72 h ($n = 3$), and 96 h ($n = 3$) p.i., and an enzyme-linked immunosorbent assay (ELISA) for CXCL10 was performed (R&D Systems, Minneapolis, MN). This analysis revealed an increase in the amount of secreted CXCL10 in VZV-infected DRG versus mock-infected DRG at all three time points p.i., with statistical significance confirmed at 72 h p.i and 96 h p.i., where three independent biological replicates were performed (Fig. 2). From 48 h p.i. to 96 h p.i., the level of CXCL10 protein remained high in infected DRG culture supernatants, with averages ranging from 400 pg/ml to 506 pg/ml. In contrast, the level of CXCL10 protein in mock-infected DRG supernatants decreased from 183 pg/ml at 48 h p.i. to 38 pg/ml by 96 h p.i. As human foreskin fibroblasts (HFFs) were used as a cell-associated inoculum, supernatants from mock- and VZV-infected HFFs were also assessed by ELISA for CXCL10. Expression in these HFFs remained below the limit of detection (12.5 pg/ml), demonstrating that ganglionic cells were the source of the CXCL10 detected in supernatants from VZV-infected DRG.

As CXCL10 can be induced by type I (α and β) and type II (γ) interferon (IFN) (12, 16), ELISA was performed (PBL Biomedical, Piscataway, NJ) to determine whether VZV induced these IFNs. At all time points p.i., IFN- α , - β , and - γ levels in supernatants from VZV-infected DRG showed no evidence of induction, but rather remained close to or below the limit of detection (25 pg/ml) (Fig. 2B to D). These data suggest that IFN induction is not a prominent feature of VZV infection of explant DRG, suggesting that an alternative mechanism may be responsible. However, our findings do not eliminate the possibility that localized IFN production (not detected in culture supernatants) may play a role in driving CXCL10 production. The processes which underpin the up-regulation of CXCL10 during VZV infection of DRG remain to be determined, and this will be an important component of future studies. This will be particularly important in naturally infected DRG as it is possible that infiltrating immune cells (e.g., T cells) reported in ganglia following reactivation *in vivo* (5) may express IFN and so contribute to the induction of CXCL10.

To elucidate the cell type(s) producing CXCL10, mock- or VZV-infected DRG were incubated for 72 h and exposed to GolgiPlug (BD, Australia) for the last 8 h. Five-micrometer sections were immunostained for CXCL10 and either the VZV early gene product pORF29; a satellite cell marker, S100b (4); or a neuronal cell marker, synaptophysin (22). Bound anti-CXCL10 antibody (Santa Cruz Biotechnology, Santa Cruz, CA) was detected with anti-mouse Alexa Fluor 594 (Invitrogen, Australia), and pORF29, S100b (Dako, Australia), and synaptophysin (Invitrogen, Australia) antibodies were detected with anti-rabbit Alexa Fluor 488. CXCL10-positive cells were observed in both mock- and VZV-infected DRG; however, in VZV-infected DRG, the CXCL10-positive cells were more abundant (Fig. 3A and B). These findings were consistent with

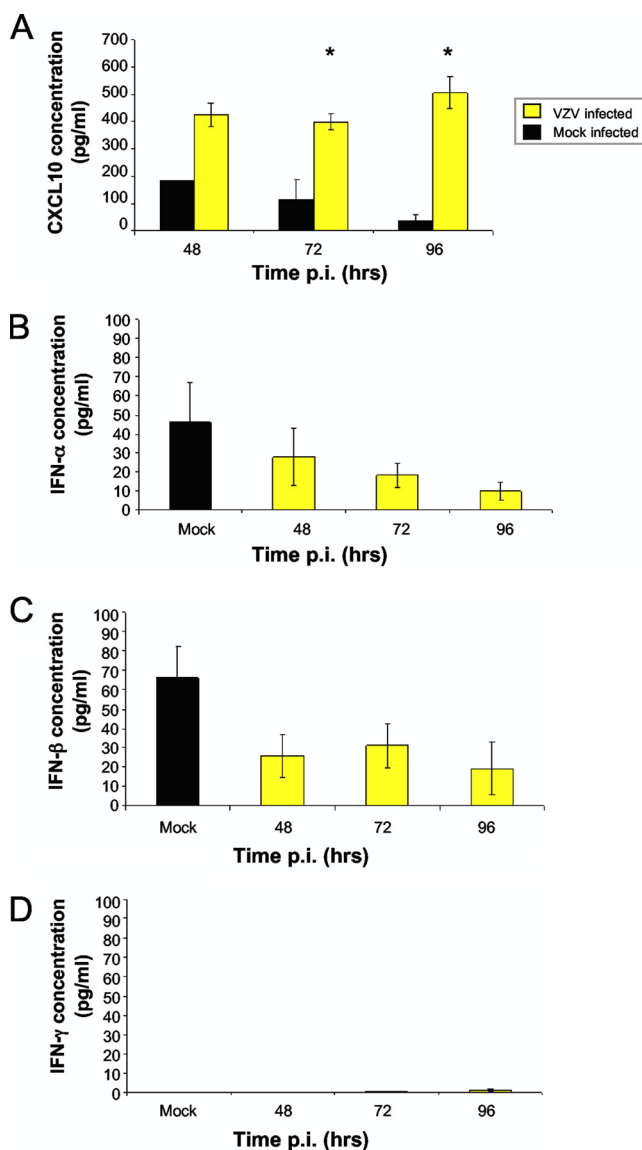


FIG. 2. Secreted CXCL10 protein levels in human ganglia experimentally infected with VZV. (A) Supernatants from mock- and VZV-infected explant ganglia were tested for CXCL10 by ELISA at 48, 72, and 96 h postinfection. Error bars represent the standard error of the mean from three independent experiments (with the exception of CXCL10 with mock infection 48 h p.i., for which $n = 1$). Significant differences from the mock-infected controls were determined for the time points where $n = 3$, using a one-tailed, paired Student's t test (*, $P < 0.05$). (B to D) Supernatants from mock- and VZV-infected explant ganglia were also tested for IFN- α , - β , and - γ by ELISA. The values for the mock infection are shown as an average from supernatants collected at all three time points. Error bars represent the standard error of the mean from three independent experiments.

the elevated levels of CXCL10 mRNA and secreted protein detected in VZV-infected DRG (Fig. 1B and Fig. 2).

The majority of CXCL10-positive cells in VZV-infected DRG costained for synaptophysin (Fig. 3D), with only sporadic costaining for S100b (Fig. 3E), demonstrating that neurons were the main source of CXCL10. In sections costained for CXCL10 and pORF29, only a few scattered cells were dually positive, with most CXCL10-positive cells showing no

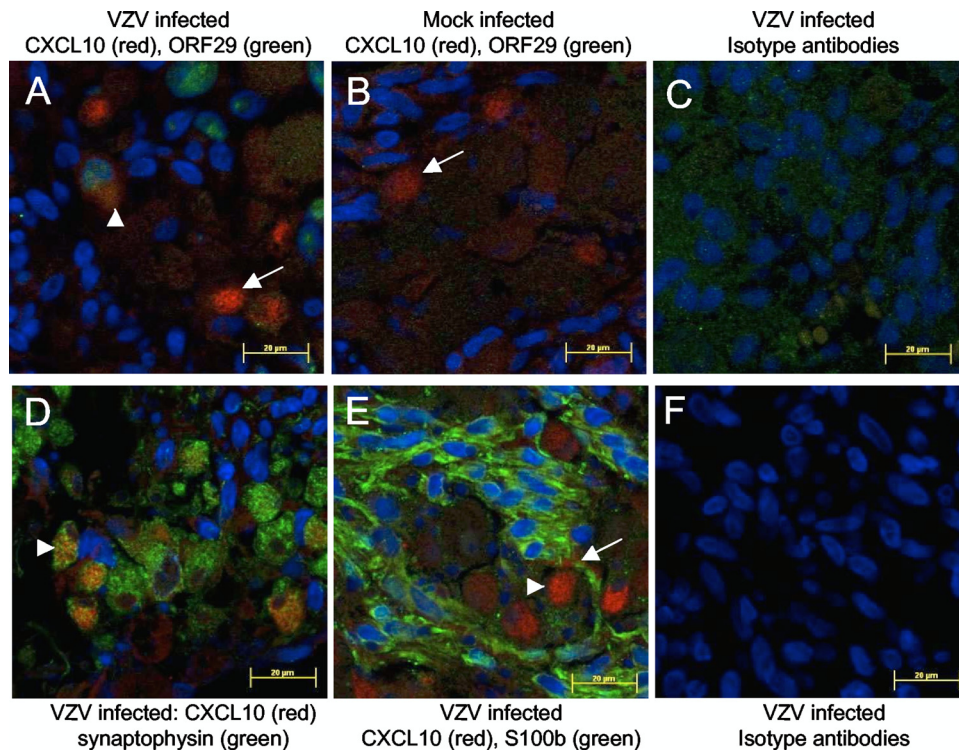


FIG. 3. Identification of cell types producing CXCL10 following experimental VZV infection of human ganglia. (A to C) Dual-immunofluorescence staining for cytoplasmic CXCL10 (red) and nuclear VZV pORF29 (green) was performed on mock- and VZV-infected ganglia treated with GolgiPlug. CXCL10-positive cells were observed in both VZV-infected (A) and mock-infected (B) ganglia. (A) VZV pORF29 was only detected in VZV-infected ganglia, and in these ganglia, both pORF29-positive (arrowhead) and -negative (arrow) cells were CXCL10 antigen positive. (C) No specific CXCL10 or VZV pORF29 staining was observed in VZV-infected ganglia stained with isotype control antibodies. (D) Dual-immunofluorescence staining for CXCL10 (red) and the neuronal marker synaptophysin (green) showed dually positive cells within infected ganglia (arrowhead). (E) Dual immunofluorescence staining for CXCL10 (red) and S100b to label satellite cells (green) showed that the vast majority of CXCL10 positive cells were S100b negative (arrowhead), in VZV infected ganglia, although occasionally smaller, dually positive cells were observed (arrow). (F) No specific CXCL10, synaptophysin, or S100b staining was observed in VZV-infected ganglia stained with isotype control antibodies. Images are representative of immunofluorescence staining on ganglia from four independent experiments.

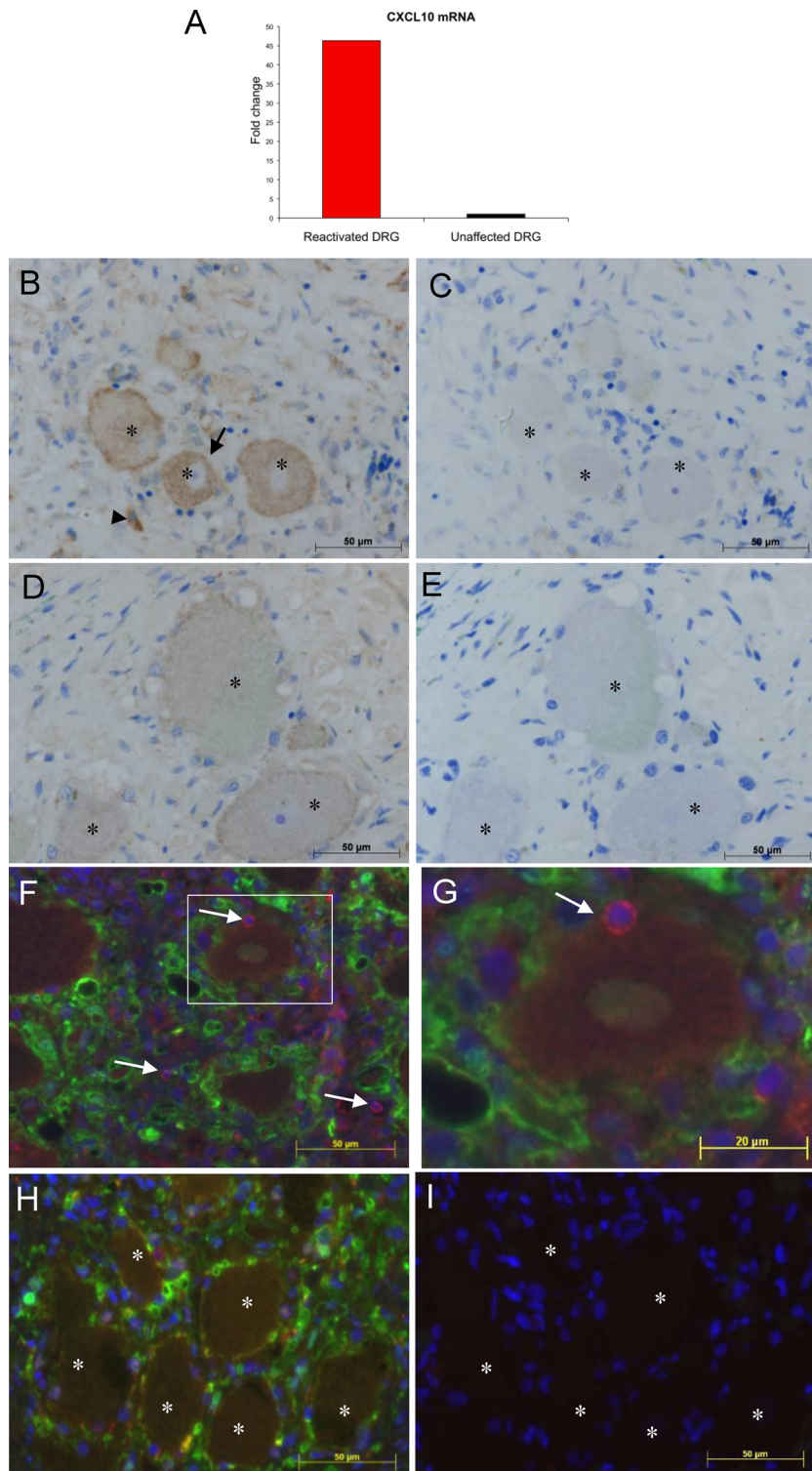
evidence of VZV infection (Fig. 3A). Taken together, these findings demonstrate that following VZV infection of DRG, CXCL10 protein is upregulated predominantly by bystander, uninfected neurons and not by the infected neurons themselves.

We next sought to determine if neurons and/or satellite cells produce CXCL10 in response to natural VZV infection. We obtained a very rare sample consisting of ganglia from a patient with herpes zoster at the time of death, but who died from unrelated causes. The patient was a 93-year-old male with dementia who died from pneumonia and had a herpes zoster rash at the left L2 dermatome at the time of death. Sections from the formalin-fixed lumbar ganglion innervating the site of the rash and an unaffected cervical ganglion from the same patient were used for nucleic acid extraction and immunohistochemistry (IHC). Both ganglia

were VZV DNA positive by PCR; however, VZV gE, which has not been shown to be expressed during latency, was detected by IHC only within the lumbar ganglion innervating the zoster rash site (data not shown), consistent with active VZV replication in the innervating ganglion and latency in the cervical ganglion.

RNA was extracted from ganglionic sections using the RecoverAll total nucleic acid isolation kit (Ambion, Carlsbad, CA) as per the manufacturer's instructions, except the protease digestion was an overnight incubation (1) and a 20-min incubation at 70°C was added following protease digestion (10). From this limited RNA, qRT-PCR was performed for CXCL10, with normalization to GAPDH. CXCL10 mRNA was detected within both ganglia; however, it was 46 times more abundant in the reactivated DRG compared to the unaffected DRG (Fig. 4A). To determine

FIG. 4. CXCL10 and CXCR3 detection in naturally infected human ganglia during herpes zoster. From a patient who died with a herpes zoster rash but not from VZV-related causes, two dorsal root ganglia (DRG) were obtained, one of which innervated the site of the lumbar rash. The other was from an unaffected cervical region. (A) The relative amount of CXCL10 mRNA was determined by qRT-PCR and normalized to the housekeeping gene coding for GAPDH. (B to E) Immunohistochemical staining of DRG sections for CXCL10. (B) The ganglion innervating



the site of the rash contained CXCL10-positive neurons (arrow) and infiltrating cells (arrowhead). (C) Staining with isotype control antibody performed on the consecutive section (corresponding neurons are indicated by asterisks) showed no specific CXCL10 staining. (D and E) Weak CXCL10 staining was observed in the unaffected DRG (D) but not in the consecutive section stained with isotype control antibody (E). (The corresponding neurons are indicated by asterisks.) Sections were counterstained with azure B to distinguish true staining from lipofuscin and neuromelanin. (F to I) Sections from the same ganglia were immunofluorescently stained for CXCR3 (red) and S100b (green) and counterstained with DAPI (4',6-diamidino-2-phenylindole) (blue). (F) Nonneuronal CXCR3-positive cells were observed throughout the reactivated lumbar DRG (arrows), with some CXCR3-positive cells juxtaposed to neurons (boxed region). Panel G shows a higher-power magnification of an inset from panel F. (H) CXCR3-positive cells were rarely detected in the unaffected DRG from the same patient. (I) Isotype control staining performed on the consecutive section to that shown in panel H showed no specific staining. (Corresponding neurons are indicated by asterisks.)

whether this increased CXCL10 mRNA expression was reflected at the protein level, 5- μ m sections were immunostained for CXCL10 by IHC, as described previously (5). Bound CXCL10 antibody (R&D Systems, Australia) was detected using a rabbit anti-goat biotin-conjugated antibody (Dako, Australia), followed by streptavidin-horseradish peroxidase (HRP), and visualized with diaminobenzidine (Dako, Australia). To distinguish specific staining from naturally occurring neuronal pigments, azure B was used as a counterstain (5, 23). Strong CXCL10 staining was clearly visible in the reactivated lumbar ganglion in both neurons and infiltrating cells (Fig. 4B). Some CXCL10 staining was detected in the unaffected cervical ganglion neurons (Fig. 4D); however, the staining intensity was markedly lower than that of the productively infected lumbar ganglion which innervated the site of the zoster rash. Counting of neurons from multiple random fields of view revealed that 48% of neurons were CXCL10 positive in the reactivated ganglion, whereas only 19% of neurons in the unaffected ganglion displayed any evidence of CXCL10 staining. No staining was observed with the isotype control antibody on consecutive sections (Fig. 4C and E). Thus, CXCL10 expression was upregulated *in vivo* in naturally infected human DRG innervating the site of the herpes zoster rash.

CXCL10 recruits memory T cells and NK cells which express CXCR3 (11, 20, 21). To determine whether cells infiltrating into DRG expressed CXCR3, we immunostained sections from the DRG innervating the herpes zoster rash and the unaffected DRG for CXCR3. Sections were also stained for S100b to better visualize resident satellite cells which provide a protective ring around neurons (6). Sudan black B was used to block neuronal autofluorescence, and staining was performed as described previously (5). Bound CXCR3 (Abcam, United Kingdom) and S100b (Dako, Australia) antibodies were detected with Alexa Fluor 595 and 488 antibodies, respectively. Numerous CXCR3-positive infiltrating cells were visible within areas of infiltration throughout the DRG innervating the site of the herpes zoster rash (Fig. 4F), including immediately adjacent to neurons (Fig. 4G). In contrast, very few CXCR3-positive cells were observed in the unaffected DRG (Fig. 4H). No CXCR3 staining was detected in neurons. Thus, *in vivo* reactivation of VZV within DRG is associated with an increase in CXCL10, together with an infiltration of CXCR3-positive cells. It is currently not possible to determine if these infiltrating immune cells are VZV antigen specific or if neurons *in vivo* are capable of presenting VZV antigens to T cells; however, the observation that some CXCR3-positive cells were immediately adjacent to neurons (Fig. 4G) raises the possibility that they may interact directly to control the spread of the virus in reactivated DRG.

In summary, we identify upregulated CXCL10 expression as a prominent feature of VZV replication in DRG during experimental infection and, most significantly, also *in vivo* during reactivation of naturally infected DRG. Furthermore, infiltrating cells expressing CXCR3, the receptor for CXCL10, were identified in DRG during VZV reactivation. CXCL10 may therefore be a signature chemokine that recruits CXCR3-positive inflammatory cells, resulting in ganglionitis. In addition to CXCL10, there are multiple other chemokines and cytokines which act as drivers of immune

cell recruitment, and these warrant further investigation to identify additional potential cellular mediators of the inflammatory response in VZV-infected DRG. In the context of CXCL10, other neurotropic viruses such as HSV, West Nile virus, and rabies virus also induce expression of this chemokine (8, 15, 17), and in the case of West Nile virus, this has been reported to drive the influx of T cells to regions of infection (8), suggesting that CXCL10 production may be a common antiviral host response to neuronal infection. This study provides the first evidence for a mechanism by which immune cells are recruited into human ganglia following natural VZV reactivation *in vivo*.

We are grateful for the assistance of Louise Cole of the Bosch Institute, the University of Sydney, for help with microscopy and Jane Radford, the University of Sydney, for assistance with histopathology. The pORF29 antibody was a kind gift from Paul Kinchington, the University of Pittsburgh.

This work was supported by a project grant from the Australian National Health and Medical Research Council.

REFERENCES

- Abramovitz, M., M. Ordanic-Kodani, Y. Wang, Z. Li, C. Catzavelos, M. Bouzyk, G. W. Sledge, Jr., C. S. Moreno, and B. Leyland-Jones. 2008. Optimization of RNA extraction from FFPE tissues for expression profiling in the DASL assay. *Biotechniques* **44**:417–423.
- Arvin, A. 2001. Varicella-zoster virus, p. 2731–2768. In D. M. Knipe and P. M. Howley (ed.), *Fields virology*, 4th ed., vol. 2. Lippincott Williams & Wilkins, Philadelphia, PA.
- Arvin, A. M. 1992. Cell-mediated immunity to varicella-zoster virus. *J. Infect. Dis.* **166**(Suppl. 1):S35–S41.
- Gowrishankar, K., B. Slobedman, A. L. Cunningham, M. Miranda-Saksena, R. A. Boodle, and A. Abendroth. 2007. Productive varicella-zoster virus infection of cultured intact human ganglia. *J. Virol.* **81**:6752–6756.
- Gowrishankar, K., M. Steain, A. L. Cunningham, M. Rodriguez, P. Blumbergs, B. Slobedman, and A. Abendroth. 2010. Characterization of the host immune response in human ganglia after herpes zoster. *J. Virol.* **84**:8861–8870.
- Hanani, M. 2005. Satellite glial cells in sensory ganglia: from form to function. *Brain Res. Brain Res. Rev.* **48**:457–476.
- Ip, P. P., and F. Liao. 2010. Resistance to dengue virus infection in mice is potentiated by CXCL10 and is independent of CXCL10-mediated leukocyte recruitment. *J. Immunol.* **184**:5705–5714.
- Klein, R. S., E. Lin, B. Zhang, A. D. Luster, J. Tollett, M. A. Samuel, M. Engle, and M. S. Diamond. 2005. Neuronal CXCL10 directs CD8⁺ T-cell recruitment and control of West Nile virus encephalitis. *J. Virol.* **79**:11457–11466.
- Kleinschmidt-DeMasters, B. K., and D. H. Gilden. 2001. Varicella-zoster virus infections of the nervous system: clinical and pathologic correlates. *Arch. Pathol. Lab Med.* **125**:770–780.
- Li, J., P. Smyth, S. Cahill, K. Denning, R. Flavin, S. Aherne, M. Pirotta, S. M. Guenther, J. J. O'Leary, and O. Sheils. 2008. Improved RNA quality and TaqMan pre-amplification method (PreAmp) to enhance expression analysis from formalin fixed paraffin embedded (FFPE) materials. *BMC Biotechnol.* **8**:10.
- Loetscher, M., B. Gerber, P. Loetscher, S. A. Jones, L. Piali, I. Clark-Lewis, M. Baggiolini, and B. Moser. 1996. Chemokine receptor specific for IP10 and mig: structure, function, and expression in activated T-lymphocytes. *J. Exp. Med.* **184**:963–969.
- Luster, A. D., J. C. Unkeless, and J. V. Ravetch. 1985. Gamma-interferon transcriptionally regulates an early-response gene containing homology to platelet proteins. *Nature* **315**:672–676.
- Mueller, N. H., D. H. Gilden, R. J. Cohrs, R. Mahalingam, and M. A. Nagel. 2008. Varicella zoster virus infection: clinical features, molecular pathogenesis of disease, and latency. *Neurol. Clin.* **26**:675–697, viii.
- Muller, M., S. Carter, M. J. Hofer, and I. L. Campbell. 2010. The chemokine receptor CXCR3 and its ligands CXCL9, CXCL10 and CXCL11 in neuro-immunity—a tale of conflict and conundrum. *Neuropathol. Appl. Neurobiol.* **6**:6.
- Nakamichi, K., M. Saiki, M. Sawada, M. Takayama-Ito, Y. Yamamoto, K. Morimoto, and I. Kurane. 2005. Rabies virus-induced activation of mitogen-activated protein kinase and NF- κ B signaling pathways regulates expression of CXC and CC chemokine ligands in microglia. *J. Virol.* **79**:11801–11812.
- Neville, L. F., G. Mathiak, and O. Bagasra. 1997. The immunobiology of interferon-gamma inducible protein 10 kD (IP-10): a novel, pleiotropic

- member of the C-X-C chemokine superfamily. *Cytokine Growth Factor Rev.* **8**:207–219.
17. **Sellner, J., F. Dvorak, Y. Zhou, J. Haas, R. Kehm, B. Wildemann, and U. Meyding-Lamade.** 2005. Acute and long-term alteration of chemokine mRNA expression after anti-viral and anti-inflammatory treatment in herpes simplex virus encephalitis. *Neurosci. Lett.* **374**:197–202.
 18. **Steiner, I., P. G. Kennedy, and A. R. Pachner.** 2007. The neurotropic herpes viruses: herpes simplex and varicella-zoster. *Lancet Neurol.* **6**:1015–1028.
 19. **Stern, J. L., J. Z. Cao, J. Xu, E. S. Mocarski, and B. Slobedman.** 2008. Repression of human cytomegalovirus major immediate early gene expression by the cellular transcription factor CCAAT displacement protein. *Virology* **378**:214–225.
 20. **Taub, D. D., A. R. Lloyd, K. Conlon, J. M. Wang, J. R. Ortaldo, A. Harada, K. Matsushima, D. J. Kelvin, and J. J. Oppenheim.** 1993. Recombinant human interferon-inducible protein 10 is a chemoattractant for human monocytes and T lymphocytes and promotes T cell adhesion to endothelial cells. *J. Exp. Med.* **177**:1809–1814.
 21. **Wald, O., I. D. Weiss, H. Wald, H. Shoham, Y. Bar-Shavit, K. Beider, E. Galun, L. Weiss, L. Flaishon, I. Shachar, A. Nagler, B. Lu, C. Gerard, J. L. Gao, E. Mishani, J. Farber, and A. Peled.** 2006. IFN-gamma acts on T cells to induce NK cell mobilization and accumulation in target organs. *J. Immunol.* **176**:4716–4729.
 22. **Zerboni, L., M. Reichelt, C. D. Jones, J. L. Zehnder, H. Ito, and A. M. Arvin.** 2007. Aberrant infection and persistence of varicella-zoster virus in human dorsal root ganglia in vivo in the absence of glycoprotein I. *Proc. Natl. Acad. Sci. U. S. A.* **104**:14086–14091.
 23. **Zerboni, L., R. A. Sobel, V. Ramachandran, J. Rajamani, W. Ruyechan, A. Abendroth, and A. Arvin.** 2010. The expression of varicella-zoster virus immediate-early regulatory protein IE63 in neurons of latently infected human sensory ganglia. *J. Virol.* **84**:3421–3430.